IASS 2020/21 SURREY 7
International Conference on Spatial Structures 2020/21

Proceedings of the IASS Annual Symposium 2020/21 and the 7th International Conference on Spatial Structures
Inspiring the Next Generation
23 – 27 August 2021, Guilford, UK
S.A. Behnejad, G.A.R. Parke and O.A. Samavati (eds.)

Description of the origami waterbomb cell kinematics as a basis for the design of thin-walled oricrete shells

Rostislav CHUDOBA*, Alice C. NIEMEYER[a], Homam SPARTALI*, Daniel ROBERTZ[b], Wilhelm PLESKEN[a]

* Institute of Structural Concrete
RWTH Aachen University, Mies-van-der-Rohe-Str. 1, 52074 Aachen, Germany
rostislav.chudoba@rwth-aachen.de

[a] Chair for Algebra and Representation Theory
RWTH Aachen University, Pontdriesch 10-16, 52062 Aachen, Germany

[b] School of Engineering, Computing and Mathematics
University of Plymouth, Drake Circus, Plymouth PL4 8AA, United Kingdom

Abstract

We present an exact algebraic solution to model waterbomb tessellations. Given the design parameters of a single waterbomb cell we can determine the global geometry of the tessellated shell directly. Thereby the preliminary design of thin-walled folded shells with load carrying function can be streamlined. The primary focus of the paper is on symmetric folding with first steps taken to consider asymmetric folding.

Keywords: Waterbomb pattern, algebraic description, folding kinematics, shell tessellation

1. Introduction

The ability of origami folding to transform parameterized planar tessellations into spatial structures unlocks an enormous potential for the design and construction of modern, lightweight engineering structures such as thin concrete shells reinforced with carbon fabrics. The waterbomb tessellation represents a traditional origami crease pattern that has been widely studied in the past. Its kinematics provide the possibility to produce statically relevant folded shapes. In particular, its global curvature can be adjusted independently from its effective cross-sectional height. This flexibility makes the waterbomb tessellation very attractive for innovative design approaches exploiting the synergy between the structural shape and non-linear material behaviour of high-performance cementitious composites. In contrast to previous work on folded carbon concrete shells, where the simulation of the folding process was implemented using numerical form-finding methods employing optimization algorithms (Chudoba and Brakhage [2]), in this paper, we focus on an exact algebraic description of the folding kinematics of a waterbomb cell. Based on this description, a direct relation between the parameters of the base and statically relevant characteristics, i.e. global curvature and local cross-sectional height, is established. The paper also investigates the possibility to relax the currently assumed symmetries of the waterbomb base and of the folding kinematics to further enhance the design options for generally shaped shell structures. First, the symmetric folding is described, leading to a cylindrically curved surface. Asymmetric folding of a base cell is presented as a generalization that could allow tessellations with non-uniform curvature and variable cross-sectional height.

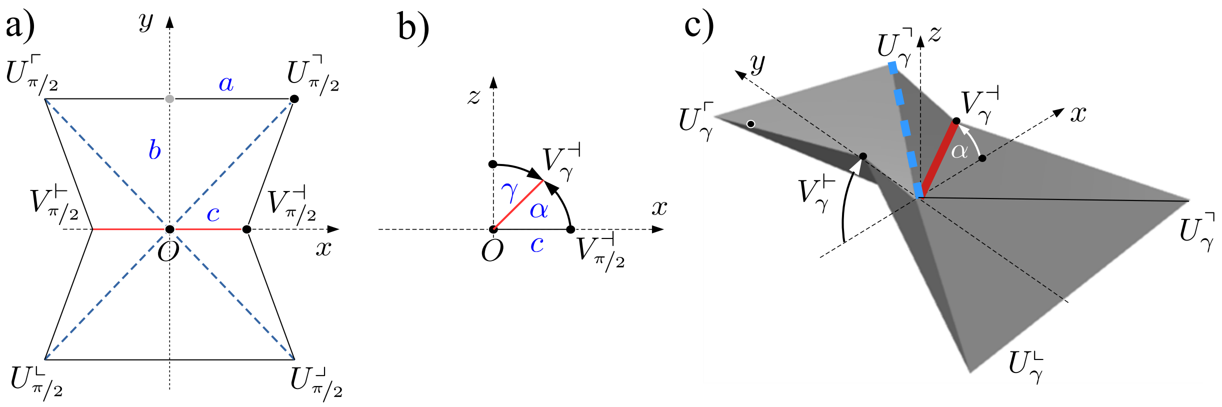

Figure 1: Waterbomb cell configuration

Related work algebraically describing the waterbomb cell kinematics has been presented in Chen et al. [1] demonstrating that in certain situations two possible symmetric folding paths can be followed. Even though general efficient numerical approaches to simulation of rigid origami have been presented during the past two decades (Zhao et al. [3], Liu and Paulino [4]), exact solutions for particular design questions are desirable to provide direct mappings between the parameters of the origami tessellation and the designed shapes.

The development of closed form descriptions of the folding kinematics and geometric characteristics presented in this paper aims to establish direct mappings between the waterbomb cell parameters on the one hand, and global curvature and effective cross-sectional height on the other. By providing statically relevant geometrical parameters, this description serves as a support of innovative design and manufacturing methodology using high-performance composite materials that combine foldable fabric reinforcement, i.e. carbon, glass and basalt, to produce customizable thin-walled folded concrete shells (Van der Woerd et al. [7], Van der Woerd et al. [8]).

2. Modelling the waterbomb base cell

We assume that the base region consists of rigid material and is composed of two trapezoids as depicted in Figure 1(a) and that the lengths a, b, and c as indicated in the figure are all positive. When the base region is placed flat in the xy-plane such that the centre is the point $O=[0,0,0]$ and the two sides of length $2a$ are parallel to the x-axis, we can observe that the pattern admits two symmetries, namely a reflection along the x-axis and a reflection along the y-axis. The mountain fold lines are on the x-axis (red line) and the valley folds on the lines $y=\frac{b}{a}x$ and $y=-\frac{b}{a}x$ (dashed blue lines), see Figure 1(a).

As shown in Figure 1, the folding state is controlled by the angle γ between the z-axis and each of the mountain fold lines. In the unfolded state, $\gamma=\pi/2$. We define the following special points, which we will refer to as the *vertices*, of the unfolded base region:

$$\begin{array}{rclrcl} U^{\ulcorner}_{\pi/2} & := & [-a,b,0], & U^{\urcorner}_{\pi/2} & := & [a,b,0], \\ U^{\llcorner}_{\pi/2} & := & [-a,-b,0], & U^{\lrcorner}_{\pi/2} & := & [a,-b,0], \\ V^{\vdash}_{\pi/2} & := & [-c,0,0], & V^{\dashv}_{\pi/2} & := & [c,0,0] \end{array}$$

and identify the vertices with vectors in EUCLIDean 3-space.

In this paper we consider two scenarios. In Section 3 we assume that the pattern remains symmetric with respect to the xz-plane as well as with respect to the yz-plane during the entire folding process. In Section 6 we treat the more general case in which we drop the hypothesis that the pattern remains symmetric about the yz-plane, but we assume that it retains either a rotational symmetry about the origin or a reflectional symmetry about the xz-plane. Our aim is to give an accurate algebraic description of the positions of the points on the base region indicated above when the base region is folded.

To describe the situation, we let 2γ denote the angle between the two mountain fold lines of the folded pattern. As we assume that the pattern remains symmetric with respect to the xz-plane, we denote by

$$\begin{array}{rcl rcl} U_\gamma^{\ulcorner} &=& [x^{\ulcorner}, y^{\ulcorner}, z^{\ulcorner}], & U_\gamma^{\urcorner} &=& [x^{\urcorner}, y^{\urcorner}, z^{\urcorner}], \\ U_\gamma^{\llcorner} &=& [x^{\ulcorner}, -y^{\ulcorner}, z^{\ulcorner}], & U_\gamma^{\lrcorner} &=& [x^{\urcorner}, -y^{\urcorner}, z^{\urcorner}], \\ V_\gamma^{\vdash} &=& [-c\sin(\gamma), 0, c\cos(\gamma)], & V_\gamma^{\dashv} &=& [c\sin(\gamma), 0, c\cos(\gamma)] \end{array}$$

the positions of the vertices of the base region in EUCLIDean 3-space when the folding angle between the z-axis and each of the mountain fold lines is γ. When $\gamma = \pi/2$. the pattern is flat in the xy-plane.

3. Waterbomb base kinematics with four parameters

In this section we assume that the base region remains symmetric with respect to the xz-plane as well as with respect to the yz-plane during the entire folding process. Hence, we can determine $U_\gamma^{\ulcorner}, U_\gamma^{\llcorner}, U_\gamma^{\lrcorner}$ and $V_\gamma^{\vdash}$ from $U_\gamma^{\urcorner}$ and $V_\gamma^{\dashv}$ by symmetry as depicted in Figure 1(c). Their coordinates result from the equations given in Table 1. As the material is rigid, these can be derived from the fact that the angles between adjacent valley and mountain fold lines (E_1) and angles between adjacent valley fold lines (E_3) as well as distances of the corners to the origin are preserved (E_2). As the positions of the base region are known for $\gamma = \pi/2$ we now assume γ takes values in $[0, \pi/2)$, whence $\cos(\gamma) > 0$.

Table 1: Equations for the waterbomb pattern

E_1:	$c\sin(\gamma)x^{\urcorner} + c\cos(\gamma)z^{\urcorner} - ac = 0$
E_2:	$(x^{\urcorner})^2 + (y^{\urcorner})^2 + (z^{\urcorner})^2 - (a^2 + b^2) = 0$
E_3:	$-(x^{\urcorner})^2 + (y^{\urcorner})^2 + (z^{\urcorner})^2 + (a^2 - b^2) = 0$

Subtracting E_3 from E_1 yields $x^{\urcorner}$ and Equation E_1 immediately yields $z^{\urcorner}$ namely

$$x^{\urcorner} = a, \tag{1}$$

$$z^{\urcorner} = \frac{a(1 - \sin(\gamma))}{\cos(\gamma)}. \tag{2}$$

Adding E_2 and E_3 yields $(y^{\urcorner})^2 = b^2 - (z^{\urcorner})^2$, thus the positive solution reads

$$y^{\urcorner} = \frac{\sqrt{b^2\cos^2(\gamma) - a^2(1 - \sin(\gamma))^2}}{\cos(\gamma)}. \tag{3}$$

Thus, the entire folding kinematics of the symmetric waterbomb cell is described.

4. Generation of a waterbomb tessellation

Using the kinematics of the waterbomb cell, we construct the tessellated folded shell geometry. To achieve this, compatibility between cells must be ensured. The kinematics of the master cell described in Section 3 based on symmetry assumptions, enforces that the tessellated waterbomb shell is curved only in the yz-plane. This fact is exploited in the derivation of the rotation and translation operators which have to be applied to the master cell to obtain the tessellated shell geometry.

The master cell has six adjacent cells (see Figure 2(a)), two of which have their origin in the yz-plane. The other four cells are shifted in the x-direction. In the folded state, the first two cells can be obtained from the master cell by rotation around the x-axis by an angle $\pm 2\theta$. The remaining four cells are obtained from the master cell by rotation around the x-axis by angle of $\pm\theta$ followed by a shift $\pm\delta$.

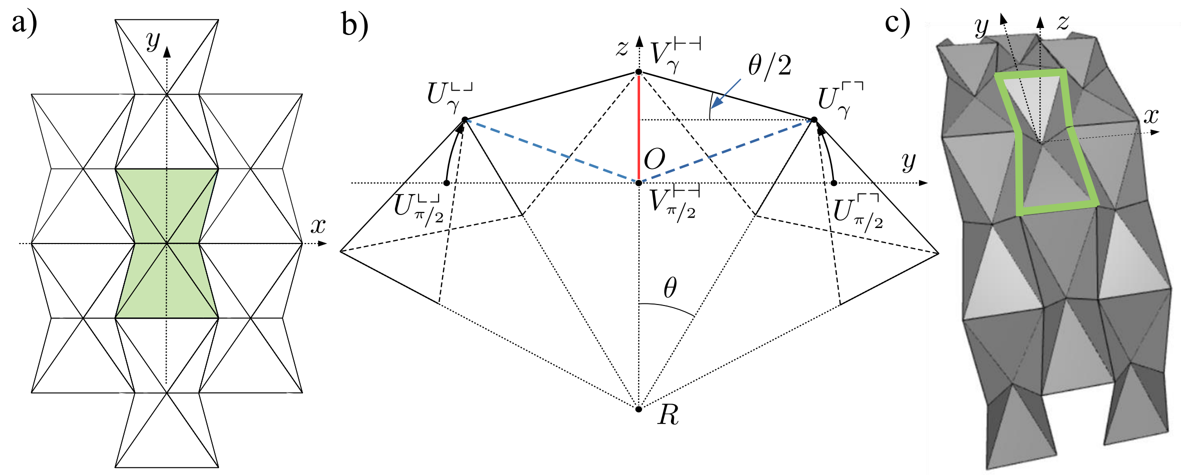

Figure 2: Cylinder shell tessellation constructed as a foldable assembly of waterbomb cells

To define the rotation operator, the angle θ needs to be expressed as a function of the design parameters a, b, c and folding angle γ. Observe that θ is the angle between the planes P_1 containing $V_\gamma^{\dashv}, U_\gamma^{\urcorner}, U_\gamma^{\ulcorner}$ and P_2 containing $V_\gamma^{\dashv}, U_\gamma^{\lrcorner}, U_\gamma^{\llcorner}$. It can be determined as follows. Let

$$N_1 = (U_\gamma^{\urcorner} - U_\gamma^{\ulcorner}) \times (U_\gamma^{\urcorner} - V_\gamma^{\dashv}) = [0, 2a(-z^{\urcorner} + c\cos(\gamma)), 2ay^{\urcorner}]$$

and

$$N_2 = (U_\gamma^{\lrcorner} - U_\gamma^{\llcorner}) \times (U_\gamma^{\lrcorner} - V_\gamma^{\dashv}) = [0, 2a(-z^{\urcorner} + c\cos(\gamma)), -2ay^{\urcorner}]$$

denote vectors perpendicular to P_1 and P_2, respectively. Thus, the equations for the planes are $P_i : (X - V_\gamma^{\dashv})N_i = 0$. The angle between P_1 and P_2 can be determined using $x^{\urcorner} = a, (y^{\urcorner})^2 = b^2 - (z^{\urcorner})^2$ and the above expression for $z^{\urcorner}$ as follows

$$\cos(\theta) = \frac{N_1 \cdot N_2}{|N_1|^2} = \frac{(z^{\urcorner} - c\cos(\gamma))^2 - (y^{\urcorner})^2}{(z^{\urcorner} - c\cos(\gamma))^2 + (y^{\urcorner})^2} \tag{4}$$

$$= \frac{c^2\cos^2(\gamma) - 2ac(1 - \sin(\gamma)) + 2\frac{a^2(1-\sin(\gamma))^2}{\cos^2(\gamma)} - b^2}{c^2\cos^2(\gamma) - 2ac(1 - \sin(\gamma)) + b^2}.$$

For $\gamma = 0$ in the maximally folded state this implies that $\cos(\theta) = \dfrac{c^2 - 2ac + 2a^2 - b^2}{c^2 - 2ac + b^2}$. Note that for $a = c$ this implies that in the totally folded state all points $V^{\vdash}_{\pi/2}, V^{\dashv}_{\pi/2}, U^{\ulcorner}_{\pi/2}, U^{\urcorner}_{\pi/2}, U^{\llcorner}_{\pi/2}$ and $U^{\lrcorner}_{\pi/2}$ lie in one plane.

Moreover, the centre $R = [0, 0, r]$ of rotation is the point on the z-axis at the same distance from the midpoints of the lines connecting $V^{\dashv}_{\gamma}$ and $V^{\vdash}_{\gamma}$ and $U^{\urcorner}_{\gamma}$ and $U^{\ulcorner}_{\gamma}$. Hence, R satisfies

$$\left| R - \frac{1}{2}(V^{\dashv}_{\gamma} + V^{\vdash}_{\gamma}) \right| = \left| R - \frac{1}{2}(U^{\urcorner}_{\gamma} + U^{\ulcorner}_{\gamma}) \right|,$$

that is $(r - c\cos(\gamma))^2 = (y^{\urcorner})^2 + (r - z^{\urcorner})^2$. Using again that $(y^{\urcorner})^2 + (z^{\urcorner})^2 = b^2$ and solving for r yields:

$$r = \frac{b^2 - c^2\cos(\gamma)}{2(z^{\urcorner} - c\cos(\gamma))} = \frac{\cos(\gamma)}{2}\frac{b^2 - c^2\cos^2(\gamma)}{a(1-\sin(\gamma)) - c\cos^2(\gamma)}.$$

Thus, the radius is:

$$|r - c\cos(\gamma)| = \cos(\gamma)\left|\frac{1}{2}\frac{b^2 - c^2\cos^2(\gamma)}{a(1-\sin(\gamma)) - c\cos^2(\gamma)} - c\right| = \frac{\cos(\gamma)}{2}\left|\frac{b^2 + c^2\cos^2(\gamma) - 2ac(1-\sin(\gamma))}{a(1-\sin(\gamma)) - c\cos^2(\gamma)}\right|.$$

With regard to Equation (1), the value of the shift δ parallel to the x-axis is obtained as

$$\delta = a + c\sin(\gamma). \tag{5}$$

With the help of the parameters θ and δ defined as functions of the cell design parameters a, b, c and folding parameter γ an arbitrarily large tessellation can be computed exactly without numerical methods. In contrast to existing numerical rigid origami models (Tachi [5], Tachi [6]), in the derived algebraic approach the positions of each cell within a shell tessellation are determined independently of all other cells, solely from the position and kinematic folding state of the master cell. The algebraic model has been implemented using the support of computer algebra systems Maple (Maple 2020[10]) and Sympy (Meurer et al. [4]), using the possibility to transform the algebraic expressions automatically to executable code. The interactive application of the model has been provided within the *Jupyter* environment based on the Python ecosystem of packages for scientific computing. An example of a fine shell tessellation with 400 cells is shown in Figure 3.

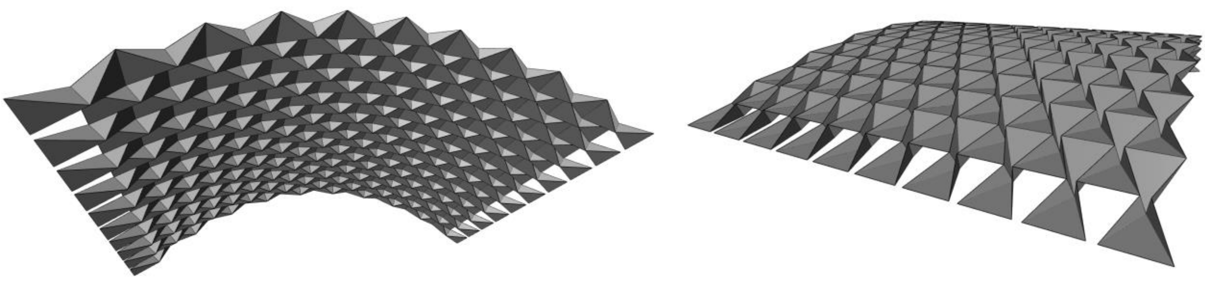

Figure 3: Two views of a tessellated shell with 20×20 cells (design parameters $\gamma = 0.2$, $\eta = 0.5$, $\zeta = 0.9$)

5. Geometric characteristics of the folded shell

With the algebraic description of the kinematics, closed form formulas can be derived that characterize the shape of folded waterbomb shells in view of their potential load carrying function. The curvature of the shell represented by the angle θ as derived in Equation (4) is depicted in Figure 4 for normalized design parameters $\eta = b/a$ and $\zeta = c/b$. For selected design parameters $(\eta,\ \zeta)$, the tessellated shells are visualized together with the corresponding planar form of their base. While the design parameter η defines the vertical slenderness of the base, choosing the parameter $\zeta < 1$ renders the waterbomb base with tailored shape and choosing $\zeta > 1$ results in bulbous shape. The study proves that folded shells with both positive and negative curvatures can be achieved. Moreover, the line of zero curvature $(\theta = 0)$ indicates the possibility to fold the crease pattern into a flat panel with a two-dimensional pattern of ribs.

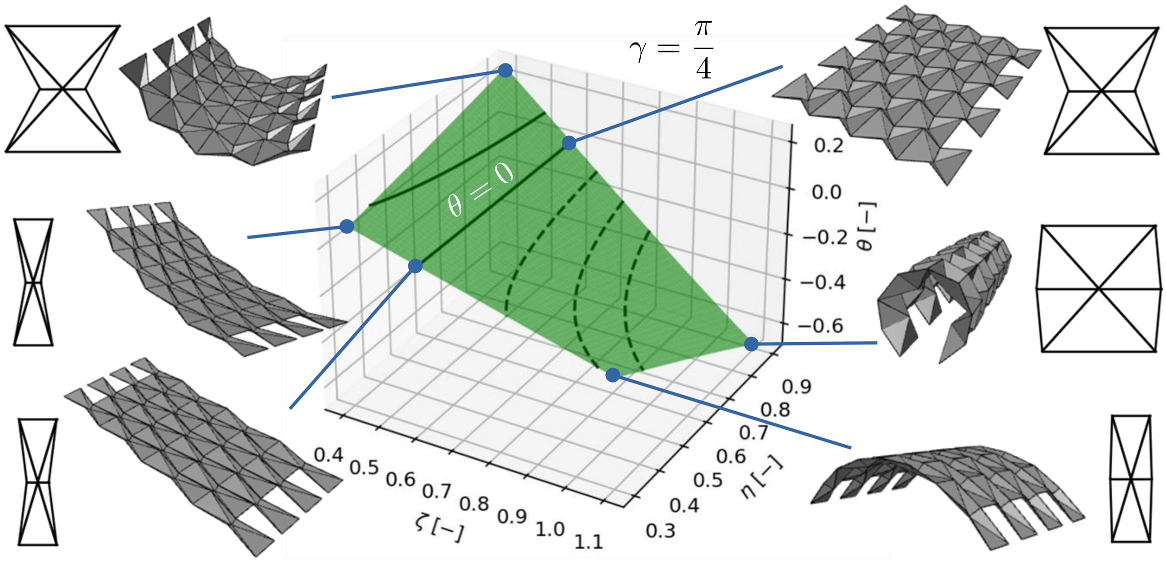

Figure 4: Cell shape parameters and corresponding shell geometry with evaluated curvatures

To construct structural elements with a sufficient local bending moment capacity, the height of the cross section, that is $z^{\urcorner} = c\cos(\gamma)$, is a relevant design parameter. An appealing feature of the waterbomb tessellation is the possibility to adjust the effective cross sectional height in a certain range independently of the global shell curvature by appropriately changing the base parameters a, b, c.

Table 2: Equations for the waterbomb pattern

$E_1:$	$c\sin(\gamma)x^{\urcorner} + c\cos(\gamma)z^{\urcorner} - ac$	$=$	0
$E_2:$	$-c\sin(\gamma)x^{\ulcorner} + c\cos(\gamma)z^{\ulcorner} - ac$	$=$	0
$E_3:$	$(x^{\urcorner})^2 + (y^{\urcorner})^2 + (z^{\urcorner})^2 - (a^2 + b^2)$	$=$	0
$E_4:$	$(x^{\ulcorner})^2 + (y^{\ulcorner})^2 + (z^{\ulcorner})^2 - (a^2 + b^2)$	$=$	0
$E_5:$	$x^{\urcorner}x^{\ulcorner} + y^{\urcorner}y^{\ulcorner} + z^{\urcorner}z^{\ulcorner} + (a^2 - b^2)$	$=$	0

6. Waterbomb cell kinematics with five parameters

We again consider the setup of Section 2. In this section we assume that the base region retains either a rotational symmetry about the origin or a reflectional symmetry about the xz-plane, but not necessarily with respect to the yz-plane during the entire folding process. Thus $U^{\llcorner}_{\gamma}$ and $U^{\lrcorner}_{\gamma}$ are determined by $U^{\ulcorner}_{\gamma}$ and $U^{\urcorner}_{\gamma}$. Similar to Section 3, we obtain the equations in Table 2 for the coordinates of the vertices because the material is rigid. More precisely, angles between adjacent valley and mountain fold lines (E_1, E_2) and angles between adjacent valley fold lines (E_5) are preserved as well as distances of the corners to the origin are preserved (E_3, E_4), where again we assume that $\gamma < \pi/2$.

Equations E_1 and E_2 immediately yield

$$z^{\ulcorner} = \frac{a - \sin(\gamma)x^{\ulcorner}}{\cos(\gamma)}, \quad z^{\urcorner} = \frac{a + \sin(\gamma)x^{\urcorner}}{\cos(\gamma)}.$$

Inserting the expressions for $z^{\ulcorner}$ and $z^{\urcorner}$ into E_3 and E_4 and solving for $(y^{\ulcorner})^2$ and $(y^{\urcorner})^2$ yields:

$$(y^{\ulcorner})^2 = \frac{b^2\cos^2(\gamma) - a^2\sin^2(\gamma) - 2a\sin(\gamma)x^{\ulcorner} - (x^{\ulcorner})^2}{\cos^2(\gamma)},$$
$$(y^{\urcorner})^2 = \frac{b^2\cos^2(\gamma) - a^2\sin^2(\gamma) + 2a\sin(\gamma)x^{\urcorner} - (x^{\urcorner})^2}{\cos^2(\gamma)}.$$

Rearranging and squaring Equation E_5 yields

$$E_6: \quad (y^{\ulcorner})^2 (y^{\urcorner})^2 = (a^2 - b^2 - x^{\ulcorner}x^{\urcorner} - z^{\ulcorner}z^{\urcorner})^2.$$

Finally, inserting the expressions for $z^{\ulcorner}$, $z^{\urcorner}$, $(y^{\ulcorner})^2$ and $(y^{\urcorner})^2$ into Equation E_6 and rearranging according to powers of $x^{\urcorner}$ yields

$$E_7: \quad A{x^{\ulcorner}}^2 + 2Bx^{\ulcorner} + C = 0,$$

where A, B and C are expressions involving $x^{\urcorner}$, namely

$$\begin{aligned}
A &= 4\sin^2(\gamma){x^{\urcorner}}^2 - 4\sin(\gamma)ax^{\urcorner} - b^2,\\
B &= 2\sin(\gamma)a{x^{\urcorner}}^2 - 2\cos^2(\gamma)a^2x^{\urcorner} + 2\cos^2(\gamma)b^2x^{\urcorner} - b^2x^{\urcorner} - 2\sin(\gamma)a^3,\\
C &= -b^2{x^{\urcorner}}^2 + 4\sin(\gamma)a^3x^{\urcorner} + 4\cos^2(\gamma)a^2b^2 - 4a^4.
\end{aligned}$$

Treating E_7 as a quadratic equation in $x^{\ulcorner}$ yields the solutions:

$$x^{\ulcorner} = -\frac{B}{A} \pm \frac{\sqrt{B^2 - AC}}{A}.$$

In particular, this allows us to express $x^{\ulcorner}$ in terms of the parameters a, b, γ and $x^{\urcorner}$.

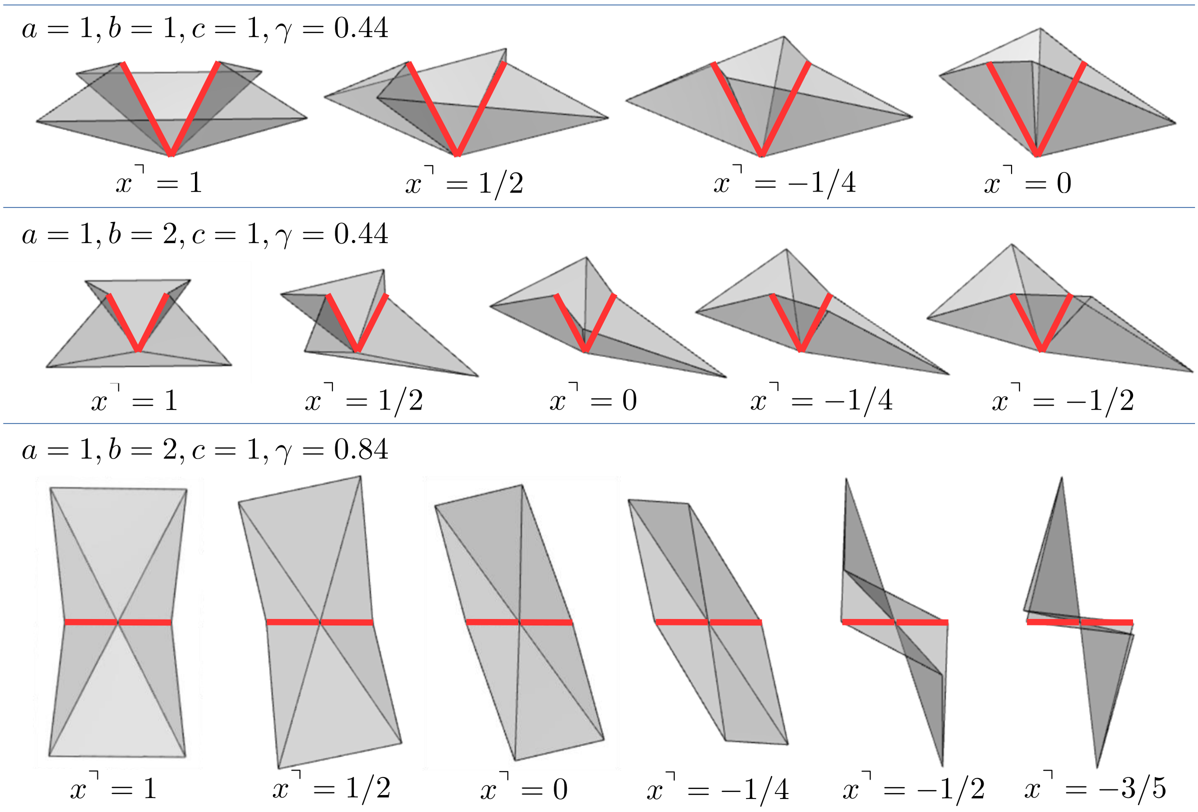

Figure 5: Asymmetrically folded waterbomb cell controlled by the displacement of $x^{\urcorner}$ exemplified for three combinations of design parameters a, b, c and control angle γ

The kinematics of the asymmetrically folded cell is controlled by the values of γ and $x^{\urcorner}$. Examples of the folding process for three selected combinations of the design parameters a, b, c and angle γ are shown in Figure 5 for decreasing values of $x^{\urcorner}$. The mountain fold lines are fixed within the xz-plane at the prescribed value of γ as highlighted in red.

7. Conclusions

An algebraic description of the waterbomb folding kinematics has been derived to support the design of thin-walled folded concrete shells made reinforced with textile fabrics.

The algebraic description allows us an exact identification of the cell vertices at any state of folding, both symmetric and asymmetric, as functions of the design and control parameters. Moreover, in the symmetric case, it facilitates the exact compatible generation of waterbomb tessellations with arbitrarily many cells from a single base cell. The assumption of facet rigidity in combination with symmetric folding induce a cylindrical geometry allowing for a construction of vault shells. The asymmetric case will be examined in future work.

With the obtained algebraic solution, statically relevant design parameters, i.e. shell curvature and effective cross-sectional height, can be directly evaluated and used in a preliminary shell design. The generated geometries serve as input for the analysis of structural behaviour of folded textile-reinforced concrete shells.

Acknowledgements
This work was funded by the Deutsche Forschungsgemeinschaft (DFG, German Research Foundation) - SFB/TRR280, Project-ID 417002380 (A04, C04). The authors acknowledge this support gratefully.

References
[1] Chen, Y., Feng, H., Ma, J., Peng, R., and You, Z., "Symmetric waterbomb origami," *Proc. R. Soc. A Math. Phys. Eng. Sci.*, vol. 472, no. 2190, Jun. 2016, doi: 10.1098/rspa.2015.0846.

[2] Chudoba, R. and Brakhage, K.-H., "Rigid-facet kinematics coupled with finite bending rotation along crease lines," in *Origami7 - Volume IV: Engineering Two*, Tarquin, Oxford, 2018.

[3] Liu, K. and Paulino, G. H., "Nonlinear mechanics of non-rigid origami: an efficient computational approach," *Proc. R. Soc. A Math. Phys. Eng. Sci.*, vol. 473, no. 2206, Oct. 2017, doi: 10.1098/rspa.2017.0348.

[4] Meurer, A. *et al.*, "SymPy: symbolic computing in Python," *PeerJ Comput. Sci.*, vol. 3, p. e103, Jan. 2017, doi: 10.7717/peerj-cs.103.

[5] Tachi, T., "Simulation of Rigid Origami," in *Origami 4*, A K Peters/CRC Press, 2009, pp. 187–200. doi: 10.1201/b10653-21.

[6] Tachi, T., "Geometric Considerations for the Design of Rigid Origami Structures," *Proc. Int. Assoc. Shell Spat. Struct. Symp. 2010*, vol. 12, no. Figure 2, pp. 458–460, 2010, doi: 10.1016/j.mpaic.2011.07.005.

[7] Van der Woerd, J. D., Bonfig, C., Hegger, J., and Chudoba, R., "Construction of a vault using folded segments made out of textile reinforced concrete by fold-in-fresh," in *Proceedings of the IASS Annual Symposium*, 2017, no. 28.

[8] Van der Woerd, J. D., Chudoba, R., and Hegger, J., "Folded bike shell-ter: Application of oricrete design and manufacturing method," in *Proceedings of the IASS Symposium: Spatial Structures in the 21st Century - Form Finding & Optimization*, 2016.

[9] Zhao, Y., Endo, Y., Kanamori, Y., and Mitani, J., "Approximating 3D surfaces using generalized waterbomb tessellations," *J. Comput. Des. Eng.*, vol. 5, no. 4, pp. 442–448, 2018, doi: 10.1016/j.jcde.2018.01.002.

[10] "Maple 2020." Maplesoft, a division of Waterloo Maple Inc., Waterloo, Ontario, 2020.